Stem Cell Research 53 (2021) 102333

Contents lists available at ScienceDirect

Stem Cell Research

journal homepage: www.elsevier.com/locate/scr

# Patient-specific iPSC-derived cellular models of LGMDR1

A.J. Mateos-Aierdi [a,b,1], M. Dehesa-Etxebeste [a,b,1], M. Goicoechea [a,b], A. Aiastui [a,b], Y. Richaud-Patin [c,d], S. Jiménez-Delgado [c,d], A. Raya [c,d,e], N. Naldaiz-Gastesi [a,b,*], A. López de Munain [a,b,f,g,*]

[a] Neuroscience Area, Biodonostia Research Institute, San Sebastian, Spain
[b] CIBERNED, Instituto de Salud Carlos III, Madrid, Spain
[c] Program of Regenerative Medicine, Bellvitge Biomedical Research Institute (IDIBELL), Hospitalet de Llobregat, Spain
[d] CIBER-BBN, Instituto de Salud Carlos III, Madrid, Spain
[e] ICREA, Barcelona, Spain
[f] Department of Neuroscience, University of the Basque Country, San Sebastian, Spain
[g] Department of Neurology, Hospital Universitario Donostia, San Sebastian, Spain

ARTICLE INFO

*Keywords:*
Induced pluripotent stem cells
LGMDR1
CAPN3
Skeletal muscle
Dystrophin

ABSTRACT

Limb-girdle muscular dystrophy recessive 1 (LGMDR1) represents one of the most common types of LGMD in the population, where patients develop a progressive muscle degeneration. The disease is caused by mutations in calpain 3 gene, with over 500 mutations reported to date. However, the molecular events that lead to muscle wasting are not clear, nor the reasons for the great clinical variability among patients, and this has so far hindered the development of effective therapies. Here we generate human induced pluripotent stem cells (iPSCs) from skin fibroblasts of 2 healthy controls and 4 LGMDR1 patients with different mutations. The generated lines were able to differentiate into myogenic progenitors and myotubes *in vitro* and *in vivo*, upon a transient *PAX7* overexpressing protocol. Thus, we have generated myogenic cellular models of LGMDR1 that harbor different *CAPN3* mutations within a human genetic background, and which do not derive from muscular biopsies. These models will allow us to investigate disease mechanisms and test therapies. Despite the variability found among iPSC lines that was unrelated to *CAPN3* mutations, we found that patient-derived myogenic progenitors and myotubes express lower levels of *DMD*, which codes a key protein in satellite cell regulation and myotube maturation.

## 1. Introduction

Limb-girdle muscular dystrophy recessive 1 (LGMDR1), previously known as LGMD2A (OMIM: 253600), is a genetically defined muscular dystrophy that presents an autosomal recessive inheritance pattern. Disease-causing mutations affect to *CAPN3* gene, which encodes the proteolytic enzyme calpain 3 (CAPN3). LGMDR1 affects 1 to 9 cases per 100,000 people, and it represents almost 30% of the LGMD cases in the population (Richard et al., 1995; Straub et al., 2018). The prevalence is considerably higher in specific regions of the world, such as the Spanish province of Gipuzkoa, where 79% of the LGMD cases are type R1, having one of the highest prevalence in the world (Urtasun et al., 1998). There are more than 500 pathogenic mutations reported to date (LOVD, 2020), and although there seems to be a correlation between the type of mutation and the severity of the disease, clinical outcome cannot be predicted yet by the mutations found in each patient (Sáenz et al., 2011). In general, the disease is clinically characterized with a slow progressive muscular weakness that affects both pelvic and scapular girdles, as well as proximal lower limb muscles (Fardeau et al., 1996). Symptoms usually appear during the second decade of life and lead to the loss of ambulation within one or two decades after onset. Despite gene therapy approaches have been tested preclinically during the last two decades, currently there are no treatments available and only palliative care can be offered to the affected patients (Straub and Bertoli, 2016).

Calpain 3 may play multiple roles in the adult skeletal muscle and it seems to be crucial for the maintenance of the sarcomere homeostasis and calcium regulation in the triads (Lasa-Elgarresta et al., 2019). However, the functional complexity of this protein hinders the

* Corresponding authors at: Neuroscience Area, Biodonostia Research Institute, San Sebastian, Spain.
*E-mail addresses:* neia.naldaiz@biodonostia.org (N. Naldaiz-Gastesi), adolfojose.lopezdemunainarregui@osakidetza.eus (A. López de Munain).
[1] Co-first authors.

https://doi.org/10.1016/j.scr.2021.102333
Received 1 September 2020; Received in revised form 12 February 2021; Accepted 31 March 2021
Available online 8 April 2021

elucidation of a clear pathological mechanism at the molecular level.

Up to date, patient muscle tissue has been very valuable to study the disease. However, biopsies are scarce and primary myoblast cultures can only be extended to a limited amount of passages. Alternatively, animal models of LGMDR1 remain as a valuable tool to understand some disease mechanisms, but they do not fully represent the disease pathophysiology due to differences in development, metabolism and genetic background, generally developing a much milder phenotype (Lostal et al., 2019).

Patient-derived induced pluripotent stem cells (iPSCs) represent a great opportunity to recapitulate disease pathogenicity in a mutation specific manner. These cells can be expanded indefinitely *in vitro*, differentiated potentially into any type of mature cell, and they also allow to develop disease-specific models, test therapeutic strategies, perform toxicity screenings and become potential sources for cell transplantation therapy (Tiscornia et al., 2011).

Myogenic differentiation of iPSCs can be achieved through exogenous expression of myogenic genes such as *MYOD* (Maffioletti et al., 2015) and *PAX7* (Darabi et al., 2012). Altered regeneration capacity and satellite cell pool have also been described in LGMDR1 patients (Rosales et al., 2013; Yalvac et al., 2017). Therefore, the *PAX7* overexpression approach was followed in order to try to recapitulate early myogenic events more accurately. Following this myogenic strategy, a CRISPR/Cas9 mediated gene correction approach has been recently developed for *CAPN3* mutations in LGMDR1 patient-derived iPSCs, where CAPN3 expression was restored in differentiated myotubes (Selvaraj et al., 2019).

In this study, we describe the generation of *in vitro* myogenic models from four LGMDR1 patient-derived iPSCs with a set of different mutations. The developed iPSC lines attain pluripotency characteristics and despite mutations in calpain 3, they are able to differentiate into myotubes both *in vitro* and *in vivo* following a transient Pax7 overexpression protocol. These models showed that calpain 3 is induced in the differentiation process towards a mature form of the culture. While the lines had a variable myogenic potential, the differences could not be directly attributed to *CAPN3* mutations. *DMD* expression was significantly reduced in patient-derived cultures, both before and after the terminal myogenic differentiation, indicating that DMD could play a role in LGMDR1. Overall, this work provides tools to advance our understanding of the pathological mechanisms of different *CAPN3* mutations in a human myogenic context and they could be used to test different therapeutic approaches to treat LGMDR1.

## 2. Methods

### 2.1. Human biological samples

Four LGMDR1 patients from the Neuromuscular Unit of Neurology Service of the Donostia University Hospital were selected to participate in this study based on the mutations in *CAPN3* gene and their disease phenotype. Patients were graded according to an adapted version of the Vignos and Archibald Scale (Walton et al., 1994). Participants signed an informed consent prior to the skin sample collection for fibroblast expansion. Two age- and sex-matched healthy donor-derived fibroblasts were obtained from the Basque Biobank to be used as controls for this study. Absence of mutations in the *CAPN3* gene was ascertained in these two samples. All procedures described here were reviewed and approved by the Ethics Committee of Clinical Investigation from Euskadi, and the Guarantee Commission for the Donation of Human Cells and Tissues at The Institute of Health Carlos III, following the guidelines of the Law 14/2007 for biomedical research.

### 2.2. Reprogramming of fibroblasts and iPSC culture

pMSCV-based retroviral vectors expressing FLAG-tagged *OCT4, SOX2, KLF4* and *cMYCT58A* were used to produce retroviruses in *Phoenix Amphotrophic* cells, as previously described (Swift et al., 1999). Cell supernatants carrying the four reprogramming retroviruses were used for infection by centrifugation at 700 *g* for 45 min at 32 °C, using 1 μg/mL of polybrene as transfection reagent. 24 h later, a second infection was performed following the same procedure. 72 h after the second infection, fibroblasts were seeded on top of irradiated feeder cells and 48 h later the medium was switched to human embryonic stem cell medium (hES medium: KnockOut DMEM medium supplemented with 20% KnockOut Serum Replacement, 2 mM GlutaMAX, 1x non-essential amino acids (NEAA) solution, 50 μM 2-mercaptoethanol, 100 U/mL penicillin, 100 μg/mL streptomycin and 10 ng/mL FGF2). This medium was replaced daily until colonies of reprogrammed cells appeared on top of the feeder cell layer. Clones were selected from each individual by expanding independent colonies. At passage 6 or higher, iPSCs were adapted to feeder-free conditions by seeding them on matrigel-coated wells and culturing them with mTeSR1 medium supplemented with 100 U/mL penicillin and 100 μg/mL streptomycin. Cells were expanded using ReLeSR reagent and culture medium was supplemented with 5 μM Y-27632 rock inhibitor for 24 h after each passage.

### 2.3. Myogenic differentiation of iPSCs

To generate myogenic progenitors, iPSCs were transduced with a doxycycline inducible *PAX7* system comprised of pSAM2-iPAX7-ires-GFP and FUGW-rtTA lentiviral vectors, as previously described (Darabi et al., 2012). To induce myogenic terminal differentiation, myogenic progenitors were plated on 0.1% gelatin-coated wells and allowed to grow to 100% confluency. Then, cells were cultured for 5 more days in differentiation medium consisting on low glucose DMEM (Gibco) supplemented with 15% KnockOut Serum Replacement (Gibco), 2 ng/mL IGF (Sigma-Aldrich) and 10 ng/mL HGF (Merck-Millipore).

### 2.4. RNA analysis

RNA was extracted with the RNeasy mini kit (Qiagen) and 1 μg of RNA was retrotranscribed using the High Capacity cDNA Reverse Transcription Kit (Applied Biosciences), following manufacturer's instructions. Dystrophin, calpain 3, *Myogenin*, *MYH3*, and *MYH2* gene expression were assessed using TaqMan probes (AppliedBiosystems) (Supp. Table 1). Analysis of *CAPN3* maturation along the differentiation process of healthy control samples was performed at day 0, 2 and 5 of differentiation. Expression results were normalized to 100%, which was calculated by summing the expression rate of the immature isoform (lacking exon 6, delta exon 6) and the mature isoform (probe for exons 5–6) at each timepoint.

### 2.5. Western blot

Differentiated cultures at day 5 were lysed in lysis buffer, protein extracts were heated at 95 °C for 3 min, and 40 μL of each protein extract were loaded into 8% acrylamide gels. Human muscle protein extracts were used as a positive control. After electrophoresis, proteins were transferred to Hibond Nitrocellulose membranes and blocked with 5% skimmed milk diluted in TBST solution shaking for 1 h at room temperature (RT). Subsequently, membranes were incubated overnight (ON) with primary antibodies (Anti-calpain 3: Cosmobio, COP-080049, 1:1000; anti-GAPDH: Cell Signaling Technology, 2118, 1:10000) diluted in 5% BSA in TBST. The following day, membranes were incubated in secondary antibody diluted in 5% skimmed milk in TBST. Finally, proteins were detected by chemiluminescence using the SuperSignal West Dura kit. Protein levels were assessed using Image Studio Lite 5.2, and standardized to GAPDH protein levels.

### 2.6. Immunofluorescence analysis

Cultured cells were fixed in 4% PFA for 10 min at RT and

permeabilized with 0.3% triton X-100 in PBS for 20 min. Next, samples were blocked with 10% donkey serum and 0.01% triton X-100 diluted in PBS for 1 h at RT, and then incubated with the primary antibody (Anti-MYHC: MF20, DSHB, 1:50; anti-Myogenin: F5D, DSHB, 1:50) diluted in PBS with 0,3% triton X-100 ON at 4 °C. The following day, cells were incubated with the secondary antibody (DonkeyαMouse –Alexa Fluor 555, Invitrogen A-31570, 1:500) diluted in PBS for 1 h at RT, protected from light. Finally, samples were incubated for 3 min in 1 μg/mL Hoechst, and mounted using the Fluorogel mounting medium (EMS).

For the detection of human iPSC-derived progenitor engraftment in the mice muscles, muscles were cryosectioned at 7 μm-thick sections. Sections were let at RT for 30 min, rehydrated in DPBS, permeabilized in 0.3% triton X-100 in DPBS for 20 min, and blocked in 3% BSA in DPBS for 1 h at RT. Samples were incubated ON at 4 °C with the primary antibody (Anti-human dystrophin NCL- DYS3, Leica; 1:20) diluted in blocking solution. The following day, samples were incubated for 1 h at RT with the second primary antibody (Anti-human lamin A/C ab108595, Abcam, 1:500), diluted in blocking solution. Thereafter, samples were incubated for 45 min at RT with secondary antibodies (DonkeyαMouse Alexa Fluor 555 Invitrogen, A-31570, 1:500; DonkeyαRabbit Alexa Fluor 488 Invitrogen, A-21206, 1:500) diluted in blocking solution. Finally, samples were incubated with 1 μg/mL Hoechst for 3 min to stain cell nuclei, and mounted with a coverslip using Fluorogel as mounting medium (EMS).

### 2.7. In vivo myogenic differentiation assessment

Transplantation of iPSC-derived muscle progenitor cells was performed on NSG (NOD.Cg- Prkdcscid Il2rgtm1Wjl/SzJ, from Charles River) mice. All procedures were performed following the guidelines and approval from Biodonostia Animal Care Committee. At 8 weeks of age, both tibialis anterior (TA) muscles were injured by injecting 7.5 μL of 100 μM cardiotoxin (Sigma) using a beveled 26G needle. The following day, patient 1 and control 2-derived $10^6$ progenitor cells at passage 4 post-sorting were transplanted into the right TA of each animal in 15 μL of volume. 15 μL of DPBS were injected into the left TA of each mouse and these muscles were used as negative controls. Mice were housed in the animal facility for 30 days before they were sacrificed.

### 2.8. Assessment of statistical significance

Statistical analysis was conducted using GraphPad Prism 5 software. An unpaired *t*-test with Welch's correction and with a 0.05 significance level was used to analyze Myogenin percentage differences. A Mann-Whitney *U* test with a 0.05 significance level was used to analyze gene expression differences. A Friedman test with a 0.05 significance level was used to assess the evolution of expression rates of each *CAPN3* isoform.

## 3. Results

### 3.1. Generation of iPSCs from healthy individuals and LGMDR1 patients.

In this study, two healthy controls and four LGMDR1 patient samples were used. Patient samples were obtained from individuals with a disease progression that ranged between intermediate and severe at the moment of the biopsy, according to the modified MVA scale. These were selected as representatives of the wide phenotypic and genetic variability found among LGMDR1 patients. Mutations in CAPN3 were heterozygous for patients 1–3, with complete gene deletions, single nucleotide mutations and deletions/insertions (delins), while patient 4 was homozygous for a delin on exon 22, the most common mutation in the Basque population with LGMDR1 (Table 1).

Primary fibroblasts at low passages derived from skin biopsies were used for reprogramming. The four Yamanaka factors *OCT4, SOX2, KLF4* and *cMYC* were expressed in the cells by infection with retroviral vectors and 3 to 6 weeks after seeding them on top of feeder cells, colonies resembling embryonic stem cell morphology were visible. iPSC colonies from each individual sample were sub-cultured and evaluated at genetic and cellular level to confirm successful reprogramming. One independent clone was selected per individual as the final iPSC line. Pluripotency was analysed in the final iPSC lines by the detection of alkaline phosphatase activity, pluripotency markers by immunofluorescence and gene expression, and the ability of the iPSC lines to differentiate into derivatives of the three primordial germ layers (Supp. Fig. 1A-D). Reprogramming of the lines was also confirmed at the epigenetic level by evaluating the methylation of CpG islands located at the promoter regions of pluripotency genes *OCT4* and *NANOG*. The iPSC lines showed 92–100% of the CpG islands unmethylated for *OCT4* and 64–95% for *NANOG* (Supp. Fig. 2A-B), indicating that these genes were not repressed at the epigenetic level as they are in differentiated cells. Finally, karyotype stability through G-banding was evaluated to circumvent any chromosomal abnormalities (Supp. Fig. 2C). STR analysis and *CAPN3* sequencing confirmed the identical genetic background of donor fibroblasts and the described iPSC clones (Supp. Info). Overall, the generated iPSC lines maintained the pluripotency state in a stable manner; they did not show any chromosomal or epigenetic abnormality and the pluripotency characteristics from healthy individual's iPSC were indistinguishable from the patient-derived ones.

### 3.2. Myogenic potential of iPSC-derived progenitors in vitro and in vivo

In order to study LGMDR1 phenotype in iPSC-derived myotubes, we performed myogenic differentiation through doxycycline inducible Pax7 overexpression (Fig. 1A). After Pax7+ cell sorting (Supp. Fig. 3), myogenic progenitors at day 0 of *in vitro* differentiation presented little expression of myogenic genes with no statistically significant differences except for embryonic myosin (*MYH3*), whose expression was increased in patient-derived progenitor cells compared to control-derived cells, but with a very low total level (Supp. Fig. 4). However, at day 5 of terminal differentiation, *in vitro* differentiated progenitors from both

**Table 1**
Summary of clinical and molecular data available from sample donors.

| Sample | Age | Sex | Origin of skin biopsy | MVA grade | Phenotype | Mutated site | DNA mutation | Protein mutation |
|---|---|---|---|---|---|---|---|---|
| Control 1 | 49 | Female | Breast | – | Healthy | – | – | – |
| Control 2 | 27 | Male | Foreskin | – | Healthy | – | – | – |
| Patient 1 | 22 | Female | Lower back | 4 | Severe | Entire gene | Complete deletion | Absent |
| | | | | | | EX24 | c.2465G > T | X822Leuext62* |
| Patient 2 | 33 | Male | Buttock | 4 | Advanced | EX11 | c.1468C > T | Arg490Trp |
| | | | | | | EX22 | 2362_2363delinsTCATCT | Arg788Serfs*14 |
| Patient 3 | 27 | Male | Proximal arm | 3 | Intermediate | EX5 | c.760A > G | Lys254GLu |
| | | | | | | EX16 | c.1910delC | Pro637Hisfs*25 |
| Patient 4 | 48 | Female | Upper back | 8 | Severe | EX22 | 2362_2363delinsTCATCT | Arg788Serfs*14 |
| | | | | | | EX22 | 2362_2363delinsTCATCT | Arg788Serfs*14 |

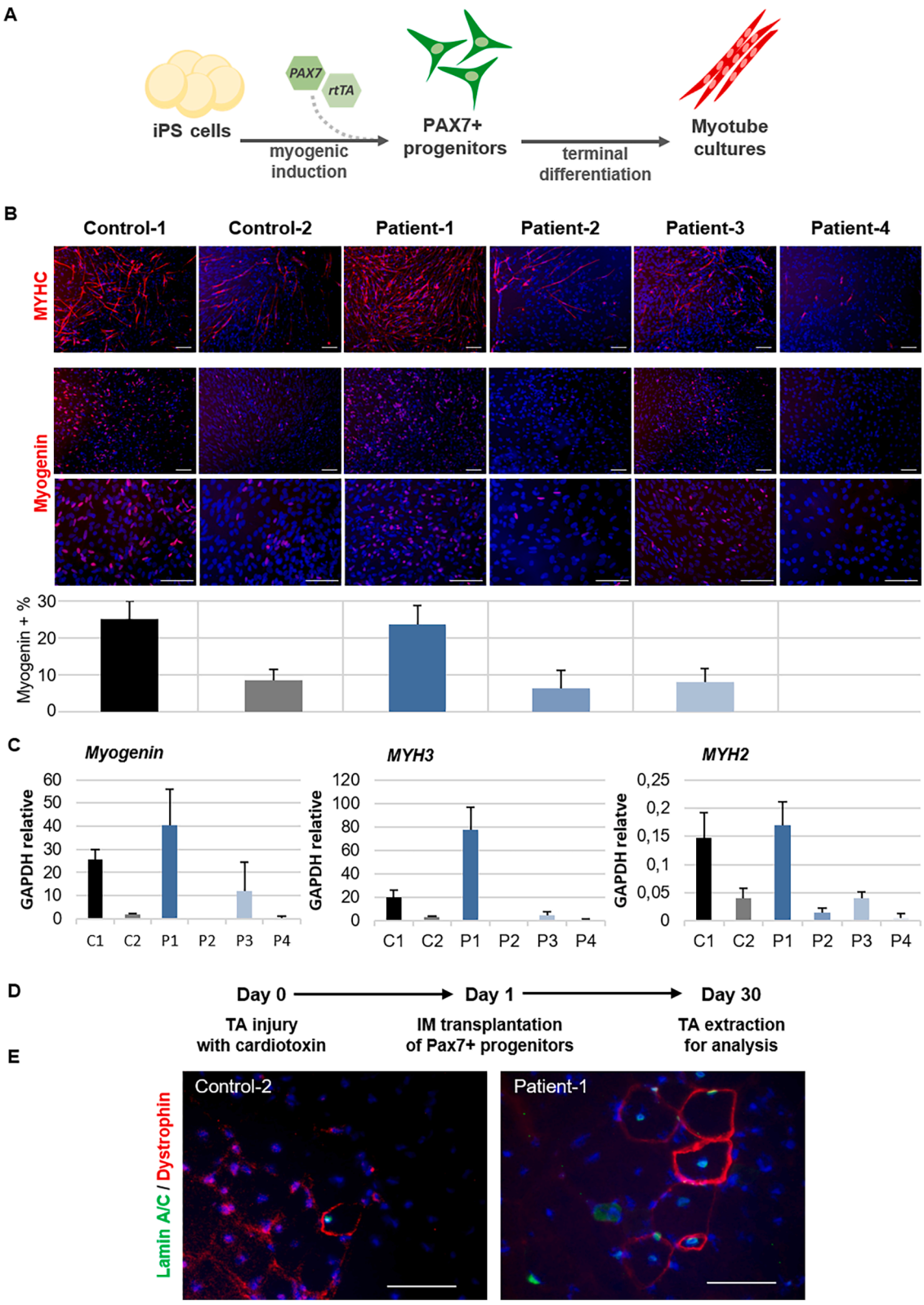


**Fig. 1.** Myogenic differentiation of iPSCs *in vitro* and *in vivo*. A) Schematic representation of the myogenic differentiation of iPSCs. B) Immunofluorescence detection of MYHC (red, line 1) and Myogenin (red, line 2 and 3) in cell cultures at day 5 of terminal differentiation, and the Myogenin positive cell quantification graphs (line 4). Scale bars: 100 μm. C) Bar graph illustrating *GAPDH*-relative myogenic gene expression rates in differentiated (day 5) cultures. D) Schematic representation of the intramuscular (IM) transplantation and regeneration experiment. E) Immunofluorescence images of TA crossections of mice transplanted with control-2 and patient-1-derived muscle progenitor cells. Detection of human lamin A/C positive cell nuclei (green) and human dystrophin-positive fibers (red). Scale bar: 50 μm. Cell nuclei are stained in Hoechst (blue). (For interpretation of the references to colour in this figure legend, the reader is referred to the web version of this article.)

control and LGMDR1 patient-derived lines were spindle-shaped and showed mature myotube protein marker expression such as Myogenin and MYHC (Fig. 1B), and *Myogenin*, *MYH3* and *MYH2* myogenic gene expression (Fig. 1C). No significative differences were observed between control and patient-derived cell lines, and a variable differentiation capacity was observed between the different cell lines, which seemed irrespective of the mutations harbored in *CAPN3* gene (Fig. 1B-C).

PAX7-expressing cells at passage 4 post-sorting were transplanted into cardiotoxin-injured TA muscles of immunodeficient mice in order to assess the *in vivo* myogenic potential of the iPSC-derived progenitors (Fig. 1D). For this experiment, patient-1 and the age matched control-2-derived cells were transplanted. 30 days after transplantation, TA muscles of injected animals were collected and analysed to assess the regenerative potential of the transplanted cells. Immunofluorescence staining of human lamin A/C allowed the detection of human cell nuclei engrafted in the mouse tissue, derived from transplanted cells (Fig. 1E). Similarly, human dystrophin expressing fibers could be detected, indicating that both control and LGMDR1 patient-derived myogenic progenitors could participate in the *in vivo* muscle fibre regeneration (Fig. 1E). In this experiment, patient-1-derived progenitors showed higher myogenic potential (data not shown), in accordance with the difference that could be observed in the *in vitro* experiment (Fig. 1B-C).

### 3.3. Calpain 3 expression in iPSC-derived cultures

Once the myogenic potential of the lines was verified, induction of calpain 3 expression was checked. At mRNA level, calpain 3 expression was assessed in control cultures and in the H9 human embryonic stem cell line, which was included as a positive differentiation control. Calpain 3 could be already detected at day 0 of differentiation, and increased at day 5 as the cultures matured in control-1 and H9 lines (Fig. 2A). This was not the case in control-2-derived cultures, which correlated with the poor differentiation potential observed in the myogenic potential assessment both *in vitro* and *in vivo* (Fig. 1B-C and D). It has been described that several splicing variants of *CAPN3* lacking exon 6 and/or exon 15 and exon 16 are detected during developmental stages, as well as during regenerative processes. This switch from immature to mature isoforms is recapitulated during *in vitro* myogenic differentiation (Herasse et al., 1999). To test this in the iPSC-derived myogenic model, the proportion of immature calpain 3 (lacking exon 6) and mature calpain 3 (including exon 6) isoforms were studied at day 0, 2 and 5 of the terminal differentiation process (Fig. 2B). The proportion of the immature isoform (lacking exon 6) was progressively reduced, while the mature form (including exon 6) increased as differentiation proceeded in control-1 and H9-derived cells. Here again, this change could not be observed in the poorly differentiating control-2-derived cells.

Then, *CAPN3* gene expression levels were analyzed by qPCR in controls and patients-derived PAX7 + progenitor cells and in terminally differentiated cultures (Fig. 2C). qPCR analysis results corroborated that *CAPN3* expression was induced following differentiation. Interestingly, *CAPN3* rates for each cell line varied greatly and they did not correlate strictly with the differentiation efficiency of each cell line (Fig. 1B). In this line, CAPN3 protein levels were assessed by western blot in *in vitro* differentiated cultures of control and patient-derived cell lines, using healthy human muscle extract as a control. The 94 KDa band corresponding to full-size calpain 3 could be detected in all the differentiated cultures (Fig. 2D). P4, which contains an homozygous mutation in exon 22, known as the Basque mutation, resulted in very low levels of 94 kDa calpain 3 band consistent with the absence of the 94 kDa calpain 3 band in muscle extracts of patients with the Basque mutation in homozygosis (data not shown). Current available calpain 3 antibodies are not completely specific and additional bands are detected, some of which are known to correspond to calpain 3 autoproteolytic products, whereas other bands might be nonspecific.

### 3.4. Reduced DMD expression in patient-derived cultures

LGMDR1 patients have an increased number of Pax7 + satellite cells as the disease progresses and fibrosis increases (Rosales et al., 2013), which indicates that satellite cell functioning and regeneration could be affected by mutations in calpain 3. Dystrophin, besides maintaining membrane integrity, it participates regulating asymmetric division of satellite cells, which is required for proper muscle regeneration. Dystrophin expression is significantly upregulated in quiescent satellite cells and it decreases upon satellite cell activation (Dumont et al., 2015).

We studied *DMD* gene expression through qPCR in our control and patient-derived cell lines and found that *DMD* gene expression was reduced in patient-derived cultures compared to healthy control-derived cultures, both in PAX7 + progenitor cells and in terminally differentiated cultures (Fig. 3).

## 4. Discussion

Despite the genetic cause of LGMDR1 has been known for more than two decades, the exact pathophysiological mechanisms by which *CAPN3* mutations lead to the disease are still unknown (Zatz and Starling, 2005). The different functions that have been attributed to calpain 3 seem to be specifically compromised by each type of mutation, and are probably affecting the disease progression. Thus, understanding the pathogenic mechanisms could help in the development of therapies. Here we show the successful generation of iPSC lines from four LGMDR1 patients with different mutations affecting calpain 3 and with a varying degree of disease progression at the time of the biopsy, as well as 2 age- and sex- matched healthy controls. The generated iPSC lines maintained genomic integrity and pluripotency characteristics in a stable manner, and differences in reprogramming efficiency among patient- and control-derived lines were not appreciated.

Despite mutations in calpain 3, patient-derived lines were able to go through a myogenic differentiation process upon Pax7 overexpression *in vitro* and *in vivo*. This myogenic protocol led to myotube maturation over time, increased calpain 3 expression, and induced its mature isoform. However, variability in the myogenic potential of the generated iPSC lines seemed to be calpain 3 independent. This was evident in the *in vitro* differentiation potential of control-1 and control-2-derived cultures-, as well as in their calpain 3 expression pattern. On the other hand, the variability observed between the patients' samples could be either due to the different mutations they harbor in *CAPN3*, or due to other technical factors related to their pluripotency level that were not detected. A possible explanation for this is that despite the exhaustive assessment of the pluripotency characteristics of the lines, it has been described that iPSCs can retain strong epigenetic marks that could directly affect their differentiation potential (Hiler et al., 2015). This means that in order to properly compare different iPSC lines, the epigenetic background should be more thoroughly analyzed and only cell lines with comparable epigenetic background should be used in comparative studies to avoid the variability derived from the epigenetic regulation.

Traditionally, DMD has been considered as a terminal differentiation and maturation marker, but it has also been described as a regulator of satellite cell activity, regulating their asymmetric division during muscle regeneration. Absence of DMD leads to a reduced generation of myogenic progenitors (Dumont et al., 2015). In LGMDR1 patients, Pax7+ satellite cells increase with disease progression and fibrosis (Rosales et al., 2013), which suggests calpain 3 could be involved in satellite cell activation and differentiation. Interestingly, DMD was found downregulated in our patient-derived lines compared to controls both in progenitor and differentiated states, which suggests DMD regulation could be also affected in LGMDR1 satellite cells, perhaps compromising the asymmetric cell division and leading to a poor regeneration and accumulation of satellite cells. At the same time, lower DMD expression in regenerating myotubes could also be affecting maturation of LGMDR1 fibers, which in patient biopsies appear irregular

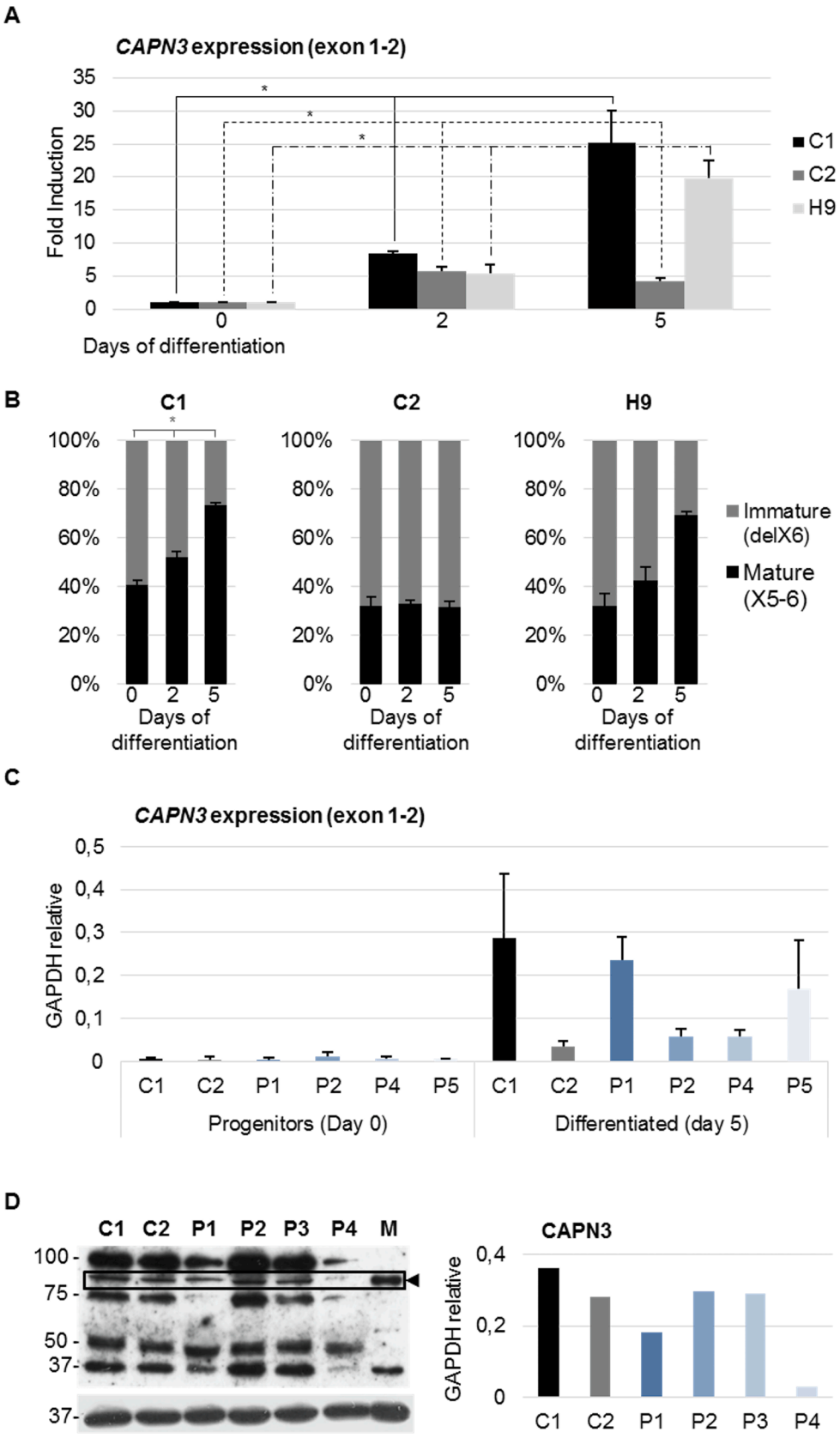


**Fig. 2.** Calpain 3 expression in iPSC-derived cultures. A) Quantification of total *CAPN3* expression (probe against exon 1–2 junction) in iPSC-derived cultures of control-1, control-2 and H9-derived cells at day 0, 2 and 5 of terminal differentiation, expressed as fold induction of the expression level at day 0. B) Percentage of immature *CAPN3* isoform (lacking exon 6) versus mature *CAPN3* isoform (including exon 6) at day 0, 2 and 5 of differentiation. Bars in A and B represent mean values and standard deviation of 3 experimental replicates. C) Bar graph illustrating *GAPDH*-relative *CAPN3* gene expression rates (probe against exon 1–2 junction) in undifferentiated (progenitors day 0) and differentiated (day 5) cultures. D) Western blot of calpain 3 protein detection using the IS2 antibody and GAPDH as endogenous control (lower blot) in protein extracts of cell cultures at day 5 of terminal differentiation, and the quantification graph. Both blots correspond to a single gel and membrane. * $p < 0.05$.

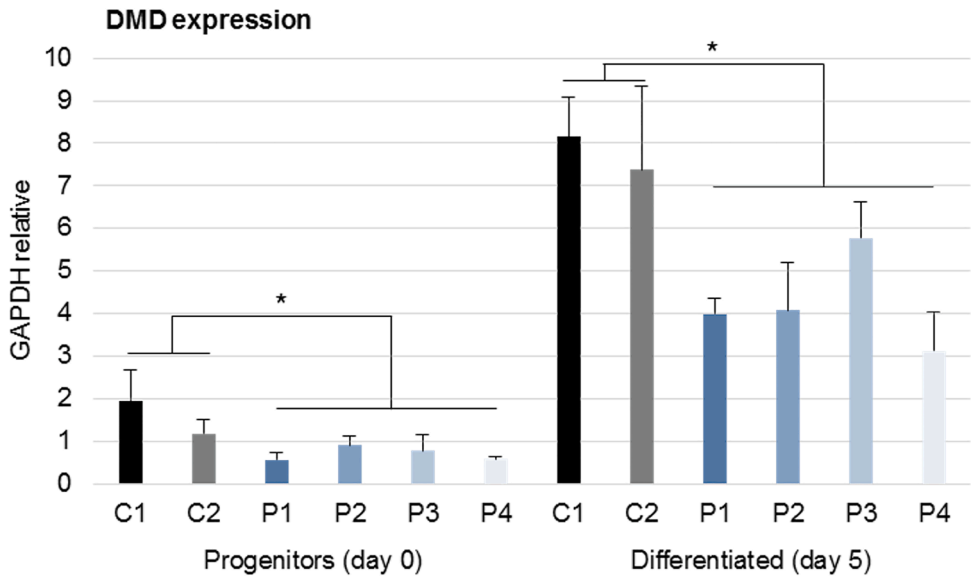


**Fig. 3.** *DMD* gene expression in iPSC-derived myogenic progenitor cells and terminally differentiated cultures. Bars graphs indicate GAPDH-relative expression rates of *DMD* gene in undifferentiated (progenitors day 0) and differentiated (day 5) cultures. Bars represent mean values and standard deviation. *p < 0.05.

in shape and variable in size (Rosales et al., 2013).

In summary, we have generated four iPSC lines from LGMDR1 patients with a set of different mutations in calpain 3, and we have shown the ability of these lines to differentiate into myogenic progenitors through a *PAX7* overexpressing myogenic protocol, and into myotubes both *in vitro* and *in vivo*. Interestingly, DMD expression was significantly reduced in patient-derived progenitors and differentiated myotubes, indicating a possible interplay between calpain 3 and DMD.

## Declaration of Competing Interest

The authors declare that they have no known competing financial interests or personal relationships that could have appeared to influence the work reported in this paper.

### *Acknowledgements*

We thank the patients and healthy individuals and their families for participating in this study donating fibroblast cells. Ethical approval for using patient samples was obtained by signed Informed Consent. We wish to thank R. Perlingeiro for providing us the Pax7-rtTA inducible system and S. Selvaraj for his technical support. We are also grateful to A. Sáenz for her support and advice and C. San José and D. Ortiz de Urbina for the support within the animal facility and the design and execution of the *in vivo* experiment.

This work has been funded by grants from Ilundain Foundation, Isabel Gemio Foundation, Fundació La Caixa, Basque Government (2015111038), Catalan Government (2017-SGR-899 and CERCA Programme), Provincial Council of Gipuzkoa (A.LdM 114/17), and Instituto de Salud Carlos III (PI14/00436, PS09/00660 and RD16/0011/0024). A.M.-A and N.N.-G. received a studentship from the Department of Education, University and Research of the Basque Government (BFI-2012-19, PRE2013-1-1168).

### *Author Contributions*

A.M.-A. elaborated hypothesis, designed and performed experiments, data interpretation and manuscript writing. M.D.-E. participated in *in vitro* experiments, data interpretation and manuscript writing. M.G. elaborated hypothesis, supervised, designed and performed *in vivo* experiments and data interpretation. A.A. Established patient cultures and provided technical support. Y.R.-P., S.J.-D., and A.R. supervised and participated in iPSC reprogramming and characterization. N.N.-G. elaborated hypothesis, designed and performed *in vivo* experiments, data interpretation and manuscript writing. A.L.d.M. participated in conception and design, data analysis and interpretation and final approval of manuscript.

## Appendix A. Supplementary data

Supplementary data to this article can be found online at https://doi.org/10.1016/j.scr.2021.102333.

## References

Darabi, R., Arpke, R., Irion, S., Dimos, J., Grskovic, M., Kyba, M., Perlingeiro, R.R., 2012. Human ES-and iPS-derived myogenic progenitors restore DYSTROPHIN and improve contractility upon transplantation in dystrophic mice. Cell Stem Cell 10 (5), 610–619.

Dumont, N.A., Wang, Y.X., von Maltzahn, J., Pasut, A., Bentzinger, C.F., Brun, C.E., Rudnicki, M.A., 2015. Dystrophin expression in muscle stem cells regulates their polarity and asymmetric division. Nat. Med. 21 (12), 1455–1463.

Fardeau, M., Hillaire, D., Mignard, C., Feingold, N., Feingold, J., Mignard, D., de Ubeda, B., Collin, H., Tomé, F.M.S., Richard, I., Beckmann, J., 1996. Juvenile limb-girdle muscular dystrophy: clinical, histopathological and genetic data from a small community living in the Reunion Island. Brain 119 (1), 295–308.

Herasse, M., Ono, Y., Fougerousse, F., Kimura, E.-I., Stockholm, D., Beley, C., Montarras, D., Pinset, C., Sorimachi, H., Suzuki, K., Beckmann, J.S., Richard, I., 1999. Expression and functional characteristics of calpain 3 isoforms generated through tissue-specific transcriptional and posttranscriptional events. Mol. Cell. Biol. 19 (6), 4047–4055.

Hiler, D., Chen, X., Hazen, J., Kupriyanov, S., Carroll, P., Qu, C., Xu, B., Johnson, D., Griffiths, L., Frase, S., Rodriguez, A., Martin, G., Zhang, J., Jeon, J., Fan, Y., Finkelstein, D., Eisenman, R., Baldwin, K., Dyer, M., 2015. Quantification of retinogenesis in 3D cultures reveals epigenetic memory and higher efficiency in iPSCs derived from rod photoreceptors. Cell Stem Cell 17 (1), 101–115.

Lasa-Elgarresta, J., Mosqueira-Martín, L., Naldaiz-Gastesi, N., Sáenz, A., López de Munain, A., Vallejo-Illarramendi, A., 2019. Calcium mechanisms in limb-girdle muscular dystrophy with CAPN3 mutations. Int. J. Mol. Sci. 20 (18), 4548. https://doi.org/10.3390/ijms20184548.

Lostal, W., Roudaut, C., Faivre, M., Charton, K., Suel, L., Bourg, N., Best, H., Smith, J.E., Gohlke, J., and Corre, G. (2019). Titin splicing regulates cardiotoxicity associated with calpain 3 gene therapy for limb-girdle muscular dystrophy type 2A. Science translational medicine 11.

LOVD, 2020. LOVD v.3.0 – Leiden Open Variation Database. https://databases.lovd.nl/shared/genes/CAPN3.

Maffioletti, S.M., Gerli, M.F.M., Ragazzi, M., Dastidar, S., Benedetti, S., Loperfido, M., VandenDriessche, T., Chuah, M.K., Tedesco, F.S., 2015. Efficient derivation and inducible differentiation of expandable skeletal myogenic cells from human ES and patient-specific iPS cells. Nat. Protoc. 10 (7), 941–958.

Richard, I., Broux, O., Allamand, V., Fougerousse, F., Chiannilkulchai, N., Bourg, N., Brenguier, L., Devaud, C., Pasturaud, P., Roudaut, C., Hillaire, D., Passos-Bueno, M.-R., Zatz, M., Tischfield, J.A., Fardeau, M., Jackson, C.E., Cohen, D., Beckmann, J.S., 1995. Mutations in the proteolytic enzyme calpain 3 cause limb-girdle muscular dystrophy type 2A. Cell 81 (1), 27–40.

Rosales, X.Q., Malik, V., Sneh, A., Chen, L., Lewis, S., Kota, J., Gastier-Foster, J.M., Astbury, C., Pyatt, R., Reshmi, S., Rodino-Klapac, L.R., Clark, K.R., Mendell, J.R., Sahenk, Z., 2013. Impaired regeneration in LGMD2A supported by increased PAX7-positive satellite cell content and muscle-specific microrna dysregulation. Muscle Nerve 47 (5), 731–739.

Sáenz, A., Ono, Y., Sorimachi, H., Goicoechea, M., Leturcq, F., Blázquez, L., García-Bragado, F., Marina, A., Poza, J.J., Azpitarte, M., Doi, N., Urtasun, M., Kaplan, J.-C., De Munain, A.L., 2011. Does the severity of the LGMD2A phenotype in compound heterozygotes depend on the combination of mutations? Muscle Nerve 44 (5), 710–714.

Selvaraj, S., Dhoke, N.R., Kiley, J., Mateos-Aierdi, A.J., Tungtur, S., Mondragon-Gonzalez, R., Killeen, G., Oliveira, V.K.P., López de Munain, A., Perlingeiro, R.C.R., 2019. Gene correction of LGMD2A patient-specific iPSCs for the development of targeted autologous cell therapy. Mol. Ther. 27 (12), 2147–2157.

Straub, V., Bertoli, M., 2016. Where do we stand in trial readiness for autosomal recessive limb girdle muscular dystrophies? Neuromuscul. Disord. 26 (2), 111–125.

Straub, V., Murphy, A., Udd, B., Group, L.W.S., 2018. 229th ENMC international workshop: Limb girdle muscular dystrophies-Nomenclature and reformed classification Naarden, the Netherlands, 17-19 March 2017. Neuromuscular disorders: NMD 28, 702.

Swift, S., Lorens, J., Achacoso, P., Nolan, G.P., 1999. Rapid Production of Retroviruses for Efficient Gene Delivery to Mammalian Cells Using 293 T Cell–Based Systems. Current protocols in immunology 31, 10.17. 14-10.17. 29.

Tiscornia, G., Vivas, E.L., Belmonte, J.C.I., 2011. Diseases in a dish: modeling human genetic disorders using induced pluripotent cells. Nat. Med. 17 (12), 1570–1576.

Urtasun, M., Saenz, A., Roudaut, C., Poza, J.J., Urtizberea, J.A., Cobo, A.M., Richard, I., Garcia Bragado, F., Leturcq, F., Kaplan, J.C., 1998. Limb-girdle muscular dystrophy in Guipúzcoa (Basque Country, Spain). Brain 121, 1735–1747.

Walton, J.N., Karpati, G., and Hilton-Jones, D. (1994). Disorders of voluntary muscle, 6th edn (Edinburgh ; New York: Churchill Livingstone).

Yalvac, M.E., Amornvit, J., Braganza, C., Chen, L., Hussain, S.-R.-A., Shontz, K.M., Montgomery, C.L., Flanigan, K.M., Lewis, S., Sahenk, Z., 2017. Impaired regeneration in calpain-3 null muscle is associated with perturbations in mTORC1 signaling and defective mitochondrial biogenesis. Skeletal Muscle 7, 27.

Zatz, M., Starling, A., 2005. Calpains and disease. N. Engl. J. Med. 352 (23), 2413–2423.